Atmos. Meas. Tech., 18, 3095–3107, 2025
https://doi.org/10.5194/amt-18-3095-2025

Atmospheric Measurement Techniques
Open Access

Radiative closure assessment of retrieved cloud and aerosol properties for the EarthCARE mission: the ACMB-DF product

Howard W. Barker[1], Jason N. S. Cole[2], Najda Villefranque[3], Zhipeng Qu[2], Almudena Velázquez Blázquez[4], Carlos Domenech[5], Shannon L. Mason[6], and Robin J. Hogan[6]

[1]Environment and Climate Change Canada, Victoria, BC, Canada
[2]Environment and Climate Change Canada, Toronto, ON, Canada
[3]CNRM, Université de Toulouse, Meteo-France, CNRS, Toulouse, France
[4]Royal Meteorological Institute of Belgium, Brussels, Belgium
[5]GMV, Madrid, Spain
[6]European Centre for Medium Range Weather Forecasts, Reading, United Kingdom

Correspondence: Howard W. Barker

Received: 31 May 2024 – Discussion started: 28 August 2024
Revised: 31 October 2024 – Accepted: 3 April 2025 – Published: 14 July 2025

Abstract. Measurements made by three instruments aboard the EarthCARE satellite, plus data from auxiliary sources, will be used synergistically to retrieve estimates of cloud and aerosol properties. The ACMB-DF processor consists of a continuous radiative closure assessment of these retrievals and is both described and demonstrated in this study. The closure procedure begins with 3D radiative transfer models (RTMs) acting on retrieved and auxiliary data. These models yield upwelling shortwave and longwave broadband radiances commensurate with measurements made by EarthCARE's multi-angle broadband radiometer (BBR). Measured and modelled radiances are averaged up to "assessment domains" that measure ~ 21 km along-track by no more than 5 km across-track, centred on the retrieved cross-section of ~ 1 km profiles, and are then combined, by angular distributions models (ADMs), to produce "effective" upwelling fluxes at top-of-atmosphere, denoted as F_{BBR} and F_{RTM}, respectively. Last, the probability $p_{\Delta\hat{F}}$ of $|F_{\mathrm{RTM}} - F_{\mathrm{BBR}}|$ being less than $\Delta\hat{F}\,\mathrm{W\,m^{-2}}$ is estimated recognizing as many sources of, assumed normally distributed, uncertainties as possible. For historical/programmatic reasons, $\Delta\hat{F}$ is set to $10\,\mathrm{W\,m^{-2}}$, but that might change during EarthCARE's commissioning phase and with Sun angle. The closure process is demonstrated up to calculation of $p_{\Delta\hat{F}}$ using four 400 km long portions of one of EarthCARE's test frames for which simulated passive measurements were computed by 3D RTMs. Note that this study, like the ACMB-DF process with real EarthCARE observations, does not comment explicitly on performance of retrieval algorithms.

1 Introduction

The EarthCARE research satellite mission, a collaborative undertaking between the European Space Agency (ESA) and the Japan Aerospace Exploration Agency (JAXA), was launched on 29 May 2024 with a payload of cloud profiling radar (CPR), backscattering lidar (ATLID), passive multispectral imager (MSI), and broadband radiometer (BBR) (see Wehr et al., 2023, for an overview). EarthCARE's overarching science goal is to estimate profiles of cloud and aerosol properties, using CPR, ATLID, and MSI measurements, sufficiently well that when operated on by broadband (BB) radiative transfer (RT) models (RTMs), simulated top-of-atmosphere (TOA) BB fluxes, for $\sim 100\,\mathrm{km^2}$ domains, are accurate to within $\pm 10\,\mathrm{W\,m^{-2}}$ (ESA, 2001; Wehr et al., 2023). *Verifying* this goal, and thus *validating* the scientific and technical choices that led to EarthCARE, requires well-defined *closure experiments*. From EarthCARE's outset, the plan has been to perform a *continuous radiative closure assessment* of its retrieved cloud and aerosol properties (ESA, 2001). The description and demonstration of this procedure is the subject of this paper.

Research satellite missions that retrieve geophysical variables usually involve verification experiments. Ideally, these experiments utilize measurements that contain information not present in measurements used to make retrievals. Often, they are made from a separate platform, such as when comparing cloud particle attributes inferred from satellite data to in situ samples from aircraft-mounted sensors that fly within the satellite's field of view (e.g., Barker et al., 2008; Deng et al., 2013; Qu et al., 2018). While in situ closure experiments provide invaluable information, they are characterized by the following: (i) logistical and interpretive difficulties (e.g., long-term plans that have to work with, and around, meteorological conditions realized over preset periods); (ii) limited spatial and temporal sampling spaces (e.g., small sampling volumes covered on short localized flights); and (iii) high operating costs that limit spatial, temporal, and sizes of samples.

Alternatives to in situ assessments use ex situ, or offsite, observations. These include (near-)simultaneous observations of atmospheric volumes made by other remote sensors located on the surface, aircraft, or satellites. In the case of satellites, sensors used for assessment can be on either a satellite of opportunity (e.g., geostationary satellite observations that coincide with those of the research satellite) or the research satellite itself. In the latter case, which is EarthCARE's, geophysical quantities retrieved by algorithms that use observations from a subset of the satellite's sensors initialize atmospheric RTMs that predict observations from an exclusive subset of sensors whose observations were *not* used by retrieval algorithms (e.g., Henderson et al., 2013; Ham et al., 2022).

Ex situ closure experiments have advantages and disadvantages relative to their in situ counterparts. The greatest advantage is the potential to continuously sample all meteorological conditions encountered throughout a mission. Moreover, while sensors that gather data for assessments incur upfront, and ongoing, data processing costs, they likely serve other purposes, too. On the other hand, the obvious disadvantage is lack of *ground-truth* sampling and the *many-to-one* problem in which key variables (e.g., ice crystal habits and sizes that could be sampled in situ) are free to range over values that lead to indistinguishable responses, thus weakening assessments. Also, it might be that measurements used to infer geophysical quantities are correlated, to some extent, with measurements used for their assessment, and this weakens assessments, too. Ultimately, the most comprehensive closure assessments of satellite retrievals involve coordinated ex situ and in situ measurements (e.g., Qu et al., 2018).

In advance of launch, ESA orchestrated a programme to numerically simulate the entire EarthCARE measurement–retrieval–assessment chain of procedures. At the front of this *end-to-end* simulation was production, by a high-resolution numerical weather prediction (NWP) model, of surface–atmosphere conditions for domains that encompass three EarthCARE *frames*, which measure 200 km across-track (i.e., the MSI's swath) by $\sim$6200 km along-track (Qu et al., 2023b). These data were then used to approximate synthetic measurements for all four of EarthCARE's sensors (Donovan et al., 2023). These "measurements" were operated on by retrieval algorithms, as summarized in several papers in this special issue, that produce EarthCARE's "best estimate" of cloud and aerosol properties. Retrieved cloud and aerosol properties are then passed to BB RTMs (Cole et al., 2023) that produce, among other quantities, BB TOA radiances that when compared to their BBR counterparts define the closure assessment and end of the initial versions of EarthCARE's virtual and real processing streams (Eisinger et al., 2024).

When dealing with synthetic ATLID, CPR, and MSI observations, the most obvious assessment of inferred geophysical variables is to compare them directly to their corresponding NWP model values (see Mason et al., 2024). Clearly, this is not possible for the actual mission whose purpose is to help improve the NWP model, and others like it, responsible for generating test data in the first place. The present report is consistent with the actual mission in that it stops at description and demonstration of the ex situ closure assessment as described above.

One of EarthCARE's many novelties is operational use of 3D RTMs in addition to the usual 1D approximations (Cole et al., 2023). Figure 1 shows shortwave (SW) radiances, computed by 1D and 3D RTMs, that correspond to the BBR's configuration. In this case, but not all cases, 1D RTM imagery is "flat" (see Barker et al., 2017). On the energetic side, differences between 1D and 3D RTM heating rates (not shown) can be striking, so for EarthCARE, BB SW flux profiles will be calculated by 3D RTMs (Cole et al., 2023).

For the current study, 3D RTMs (Villefranque et al., 2019, 2022) were used to simulate MSI and BBR measurements for use in the virtual system, which until now had relied on radiance observations simulated by 1D RTMs (see Donovan et al., 2023; Mason et al., 2023). Due to computational limitations, 1D and 3D RT radiances were produced for just four domains measuring 400 km along-track by 30 km across-track, at 250 m horizontal resolution. Their differences demonstrate the need for realistic radiances in both *end-to-end* simulations and the mission proper.

The following section describes EarthCARE's radiative closure assessment procedure, which defines the so-called ACMB-DF processor. The third section discusses use of synthetic passive measurements created by 3D, rather than the usual 1D, RTMs. This is followed by application of the closure process to synthetic measurements. A summary and conclusions are presented in the final section.

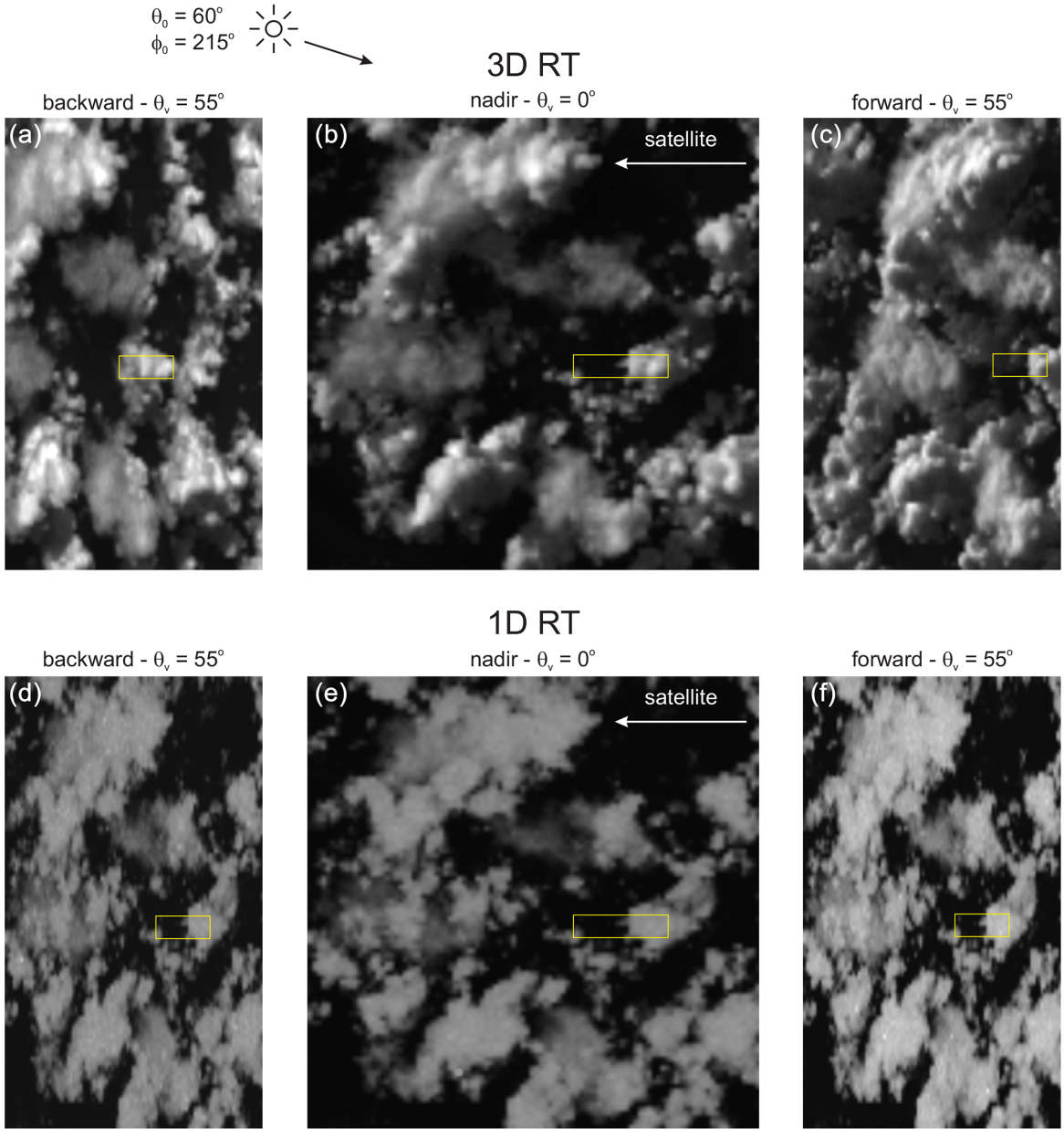

Figure 1. Panels **(a)**, **(b)**, and **(c)** show BB SW radiances, simulated by a 3D RTM, as observed by the BBR's backward-, nadir-, and forward-pointing telescopes. Viewing zenith angle θ_v for off-nadir views is 55°. The entire image is 100×100 km. Yellow rectangles indicate the size of 5×21 km assessment domains. Lower panels are the same except radiances were simulated by a 1D RTM. For both simulations solar zenith and azimuth angles were $\theta_0 = 60°$ and $\varphi_0 = 215°$, respectively; φ_0 is clockwise from the north with the satellite tracking due south (see Qu et al., 2023b). Radiances were co-registered at cloud top, or ∼ 17 km.

2 EarthCARE's continuous radiative closure experiment

2.1 Overview

Geophysical variables retrieved from observations made by EarthCARE's ATLID, CPR, or MSI sensors are referred to as L2 products (see Wehr et al., 2023, and Eisinger et al., 2024, for overview summaries). Products arising from a single sensor's data are designated as L2a, while those from multiple sensors are L2b. L2 products are reported on all or part of the Joint Standard Grid (JSG), which has a horizontal resolution of ∼ 1 km and, looking forward along the satellite's motion vector, extends across-track 35 km to the right and 115 km to the left; the asymmetry helps reduce complications that arise from sunglint. Vertically resolved L2 variables are on 0.1 km thick layers, extend from surface to 20 km, and form the L2

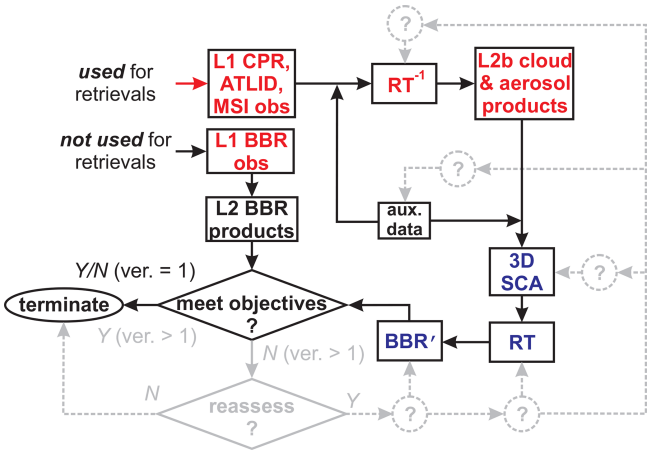

Figure 2. Flowchart showing EarthCARE's radiative closure assessment programme. Version 1 (ver. = 1) represents EarthCARE's initial processing plan. It terminates unconditionally after comparing modelled to measured BBR quantities whilst reporting the likelihood of their difference being within $\pm 10\,\mathrm{W\,m^{-2}}$. For subsequent processing (ver. > 1), it is expected that if modelled and measured BBR quantities compare unsatisfactorily, potentially all steps in the processing chain will be interrogated and adjusted until some level of agreement is reached.

plane. The focus of radiative closure assessments is on L2b profiles of cloud and aerosol properties.

Figure 2 summarizes the flow of products leading to, and including, EarthCARE's ex situ radiative closure experiment. It begins with L2b variables and auxiliary information, from model analysis (see Eisinger et al., 2024) and climatological statistics (Qu et al., 2023b), being used by the 3D Scene Construction Algorithm (SCA) (Barker et al., 2011; Qu et al., 2023a). Using MSI radiances, the SCA associates an off-nadir JSG pixel with its closest matching nadir pixel. L2b profiles, as well as surface properties, associated with the donor nadir column get replicated at the off-nadir recipient to form a 3D surface–atmosphere system around, and consisting entirely of data in, the L2 plane.

Information from the SCA gets ingested into various forward radiative transfer models (Cole et al., 2023) that predict profiles of BB radiative fluxes as well as upwelling BB radiances at TOA that are commensurate with BBR observations. The essence of the closure assessment, which marks the end of version 1 of EarthCARE's production chain, is the comparison of TOA *effective fluxes* that derive from modelled and measured radiances averaged over assessment domains (ADs). Following Qu et al.'s (2023a) notation, assessment domains consist of n_{assess} JSG pixels along-track with across-track half-widths of m_{assess} JSG pixels, for a total of $(2m_{\mathrm{assess}}+1)\,n_{\mathrm{assess}}$ JSG pixels. The current plan (Qu et al., 2023a) is $n_{\mathrm{assess}} = 21$ and $m_{\mathrm{assess}} = 2$ so that assessment domains will measure $\sim 5 \times 21$ km.

2.2 Closure assessment variable

The most direct closure assessments use the BBR's three directional radiances. Nadir BBR radiances, by themselves, provide weak closure tests, for as shown elsewhere (e.g., Barker et al., 2014), both SW and LW BB nadir radiances can be correlated well with MSI radiances that are used by some L2 retrieval algorithms (e.g., Mason et al., 2023). Off-nadir BBR radiances have viewing geometries that differ markedly from all other EarthCARE sensors, are usually much less correlated with MSI nadir radiances than are BB nadir radiances, and so have the potential to provide stringent radiative closure assessments. There is always, however, the possibility that substantial fractions of photons that constitute off-nadir BBR radiances have trajectories that depend much on atmospheric attenuators and surfaces outside the AD. This happens when cloud and aerosol occur between the BBR and AD, and when bright clouds or surfaces backlight an AD. In extreme cases, off-nadir radiances might say very little about the quality of retrievals within the AD (Barker et al., 2015; Tornow et al., 2015).

Another issue with direct use of radiances is that it breaks with EarthCARE's long-held science goal that states explicitly that retrieval quality be gauged in terms of $\mathrm{W\,m^{-2}}$ (ESA, 2001; Illingworth et al., 2015; Wehr et al., 2023). To abide by this, the obvious approach is to compare TOA fluxes predicted by ACM-RT's RTMs to corresponding values obtained by EarthCARE's angular distribution models (ADMs) (Velázquez Blázquez et al., 2024), which for the SW are based on CERES ADMs (Kato and Loeb, 2005; Domenech and Wehr, 2011) and for the LW on the operational GERB LW flux estimation (Clerbaux et al., 2003a, b). Once outside the idealized world of 1D RT, however, defining TOA fluxes for 5×21 km or smaller atmospheric columns is fraught with ambiguity and potentially large and difficult to quantify uncertainties (cf. Kato and Loeb, 2005).

For these reasons, it was decided that the most well-defined, reliable, and programmatically satisfying way to perform radiative closure assessments is to transform "both" BBR measured and ACM-RT simulated TOA BB radiances into "effective fluxes" via EarthCARE's ADMs. The attraction of using $F_{\mathrm{RTM}} - F_{\mathrm{BBR}}$, where F_{RTM} and F_{BBR} are effective fluxes derived from either an RTM's or the BBR's radiances, for the closure assessment variable is that it largely sidesteps uncertainties associated with instantaneous application of ADMs and complications around exact definition of TOA fluxes. It does mean, however, that true "fluxes" never enter EarthCARE's closure assessments and that potential issues associated with the use of off-nadir radiances, as mentioned above, go unaddressed (at least for EarthCARE's initial processing).

Following Velázquez Blázquez et al. (2024), longwave effective fluxes are defined as

$$F_{\mathrm{BBR}} = \frac{1-\alpha}{2}\left[f_{\mathrm{BBR}}(1) + f_{\mathrm{BBR}}(3)\right] + \alpha\, f_{\mathrm{BBR}}(2)\,, \qquad (1)$$

where flux estimates from each telescope are

$$f_{\mathrm{BBR}}(i) = \frac{\pi L_{\mathrm{BBR}}(i)}{R(i)}, \tag{2}$$

where $\alpha = 1/3$, $L_{\mathrm{BBR}}(i)$ are unfiltered BBR radiances ($\mathrm{W\,m^{-2}\,sr^{-1}}$), in which $i = 1$, 2, and 3 correspond to forward, nadir, and backward viewing, respectively, and $R(i)$ denotes parameterized anisotropic factors that depend on MSI brightness temperatures. Model-generated counterparts of Eq. (1), designated as F_{RTM}, are computed the same way except that Monte Carlo-estimated radiances L_{RTM} replace L_{BBR} in Eq. (2) (see Cole et al., 2023).

Shortwave effective fluxes are more difficult to define than for LW because of pronounced anisotropy. Following Velázquez Blázquez et al. (2024), ADM-based fluxes derived from the nadir, aft, and fore views are combined as

$$F_{\mathrm{BBR}} = \left[\sum_{i=1}^{3} \frac{\delta(i)}{\varepsilon_{f_{\mathrm{BBR}}(i)} \pi \varepsilon_{R(i)}}\right] \left[\sum_{i=1}^{3} \frac{\delta(i) f_{\mathrm{BBR}}(i)}{\varepsilon_{f_{\mathrm{BBR}}(i)} \pi \varepsilon_{R(i)}}\right], \tag{3}$$

where $f_{\mathrm{BBR}}(i)$ is as in Eq. (2), but the anisotropic factors for each view are obtained from an artificial neural network trained with surface and atmospheric analysis data, and $\varepsilon_{f_{\mathrm{BBR}}(i)}$ and $\pi\varepsilon_{R(i)}$ are flux uncertainties arising from the ADMs and the BBR unfiltered radiance estimation (Velázquez Blázquez et al., 2024), respectively. When all $f_{\mathrm{BBR}}(i)$ values agree to within $\pm 10\,\%$, $\delta(i) = 1$ for all i. When two $f_{\mathrm{BBR}}(i)$ values agree to within $\pm 10\,\%$, each uses $\delta = 1$ with the outlier getting $\delta = 0$. If all $f_{\mathrm{BBR}}(i)$ values differ by more than $10\,\%$, only the smallest $\varepsilon_{f_{\mathrm{BBR}}(i)} \pi \varepsilon_{R(i)}$ uses $\delta = 1$. When computing F_{RTM} with Eq. (3), 3D Monte Carlo RTM radiances L_{RTM} (Cole et al., 2023) replace L_{BBR}, and Monte Carlo radiance uncertainties $\varepsilon_{R(i)}$ replace BBR measurement uncertainties.

An optional approach is to eliminate radiance uncertainty from Eq. (3) by stochastically sampling $L_{\mathrm{BBR}}(i)$ and $L_{\mathrm{RTM}}(i)$ and producing distributions of F_{BBR} and F_{RTM}. This has the potential to sample multiple combinations of $\delta(i)$ and hence substantially broaden distributions of plausible F_{BBR} and F_{RTM}. This will be explored during EarthCARE's commissioning phase but not here.

When estimating effective flux based on the BBR's three views, an ever-present issue is co-registration of radiances to ensure that they correspond to the AD defined at nadir. In general, this requires dynamic specification of an altitude that corresponds to where the majority of photons received by the telescopes begin their final upward trajectories. For clear skies, this is (close to) Earth's surface – especially for SW radiation. For cloudy skies, however, this could be anywhere from surface to cloud top, and cloud top might be outside the AD (see Barker et al., 2014). Both here and with real measurements, specification of co-registration altitude is defined using the methodology presented in Velázquez Blázquez et al. (2024).

2.3 Closure assessment metric

We assume that "best estimates" of F_{BBR} and F_{RTM}, averaged over D, are mean values of underlying Gaussian distributions $N\left(F_{\mathrm{BBR}}, \sigma^2_{F_{\mathrm{BBR}}}\right)$ and $N\left(F_{\mathrm{RTM}}, \sigma^2_{F_{\mathrm{RTM}}}\right)$, where $\sigma^2_{F_{\mathrm{BBR}}}$ and $\sigma^2_{F_{\mathrm{RTM}}}$ are respective standard deviations and taken to be "uncertainties". Although some key input variables for ACM-RT's RTMs will have estimated uncertainties, computational limitations and time constraints (see Cole et al., 2023) mean that many contributions to $\sigma^2_{F_{\mathrm{RTM}}}$ will be neglected.

This also pertains to auxiliary variables, not inferred from EarthCARE retrievals, such as surface optical properties, and temperature and moisture profiles. Nevertheless, we define

$$\Delta F = F_{\mathrm{RTM}} - F_{\mathrm{BBR}} \tag{4}$$

and assume that pooled uncertainty can be approximated simply as

$$\sigma_p^2 \approx \sigma^2_{F_{\mathrm{BBR}}} + \sigma^2_{F_{\mathrm{RTM}}}. \tag{5}$$

Therefore, estimated probability of $|\Delta F| \le \Delta\hat{F}$ is

$$\begin{aligned} p_{\Delta\hat{F}} &= \frac{1}{\sigma_p\sqrt{2\pi}} \int_{-\Delta\hat{F}}^{\Delta\hat{F}} \exp\left[-\frac{(x-\Delta F)^2}{2\sigma_p^2}\right] \mathrm{d}x \\ &= \frac{1}{2}\left[\mathrm{erf}\left(\frac{\Delta\hat{F}-\Delta F}{\sqrt{2}\sigma_p}\right) - \mathrm{erf}\left(\frac{-\Delta\hat{F}-\Delta F}{\sqrt{2}\sigma_p}\right)\right], \end{aligned} \tag{6}$$

where $\mathrm{erf}(\cdots)$ is the error function. The quantity $p_{\Delta\hat{F}}$ provides a succinct indication of the likelihood that L2 products, and to a lesser extent auxiliary data and SCA performance, have been retrieved well enough to be designated as having satisfied the mission's goal of $\pm\Delta\hat{F}$, at the scale of the AD. Figure 3 illustrates this schematically.

The tacit assumption, thus far, has been that use of $\Delta\hat{F} = 10\,\mathrm{W\,m^{-2}}$, EarthCARE's goal, applies everywhere, all the time, though it has never been specified if this means to SW and LW radiation separately or to their sum. While this may be reasonable say "everywhere, all the time" for LW radiation, this is not the case for SW fluxes, where aiming for $|\Delta F| \le 10\,\mathrm{W\,m^{-2}}$ at small θ_0 is much more demanding than at large θ_0. What has been settled on for SW radiation is to replace $\Delta\hat{F}$ in the above equations with $\Delta\hat{F}\mu_0/\langle\mu_0\rangle$, where μ_0 is local value of $\cos\theta_0$, and $\langle\mu_0\rangle$ is arithmetic mean of μ_0 for the portion of EarthCARE's orbit with $\mu_0 > 0$.

For simplicity, $\Delta\hat{F}$, for both SW and LW, does not depend on surface or atmospheric conditions. Moreover, in practice, any value of $\Delta\hat{F}$ could be used. At the time of writing, the plan is that ACMB-DF will report values of $p_{\Delta\hat{F}}$ for $\Delta\hat{F}$ from 5 to $50\,\mathrm{W\,m^{-2}}$ in increments of $5\,\mathrm{W\,m^{-2}}$.

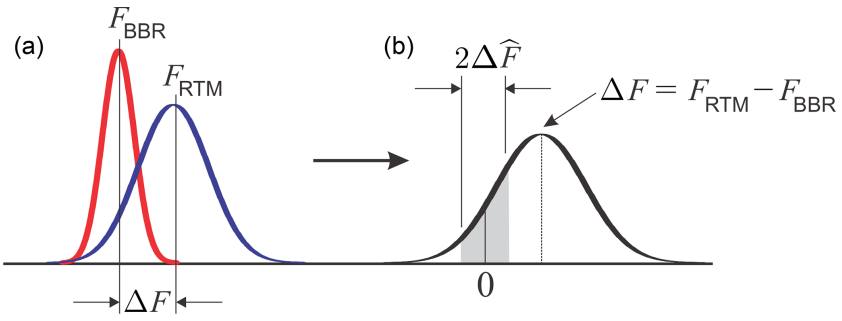

Figure 3. Schematic illustrating **(a)** assumed normalized Gaussian distributions of measured $N\left(F_{\mathrm{BBR}}, \sigma^2_{F_{\mathrm{BBR}}}\right)$ (red) and modelled $N\left(F_{\mathrm{RTM}}, \sigma^2_{F_{\mathrm{RTM}}}\right)$ (blue) fluxes and the resulting **(b)** Gaussian distribution of their difference $N\left(\Delta F, \sigma^2_p\right)$. Area of the shaded region is the probability that F_{BBR} and F_{RTM} differ by less than $\pm\Delta\hat{F}$.

3 On the use of 3D RTMs to simulate observed radiances

Simulated radiometric observations produced by 1D RTMs are often used for development and testing of cloud and aerosol retrieval algorithms (see Donovan et al., 2023, and many other papers in this special issue). For EarthCARE, 1D RTMs were needed, because of computational burden, to simulate observations for three large test frames (Qu et al., 2023b) at spectral and spatial resolutions high enough to capture radiometer filter functions and spectral unfiltering (Velázquez Blázquez et al., 2024). A better approximation of real conditions is achieved, however, when 3D RTMs are used to simulate radiances. To demonstrate the closure assessment process, all passive radiances were computed by 3D RTMs (Villefranque et al., 2019) at horizontal grid spacing of $\Delta x = 0.25$ km, which is the resolution of test frame data, for four select $\sim 400 \times 30$ km portions of the *Hawaii* frame; setting $\Delta x \to \infty$ affects 1D RT conditions commensurate with all other tests reported in this special issue.

As use of 3D RTMs to simulate observed and modelled radiances represents a marked departure from all other reports in this issue, impacts due to this change are presented briefly here. It should be noted, however, that the point of this section, and indeed the entire paper, is not to explain, or examine in detail, retrieval algorithm performances but rather to focus on the closure methodology.

Figure 4 shows the impact of constraining CAPTIVATE's synergistic retrieval algorithm (ACM-CAP; Mason et al., 2023) with MSI radiances simulated by either a 1D or 3D RTM. Scene 1 is covered by ice cloud with ice water path (IWP) generally larger than 20 g m^{-2}, save for 1 to 1.5° S where the nadir cross-section is almost ice-free. Nearby ice clouds, however, cast shadows onto low-level liquid clouds for 3D RT but not for 1D RT. Therefore, when radiances are based on 3D RT, liquid clouds appear to CAPTIVATE, which assumes 1D RT to be too thin. The other scene with upper-level ice cloud is 4, which has widespread IWP of ~ 400 g m^{-2} near 21° S and 65 g m^{-2} near 22° S. In this case, irradiance onto low liquid clouds depends little on the type of RTM, so liquid water path (LWP) values are very similar.

In contrast, scenes 2 and 3 have almost no ice cloud, so differences in retrieved LWPs stem from either side illumination or shadowing. Generally, 3D RT values are very close to or less than their 1D counterparts, implying that shadowing and entrapment of photons (cf. Hogan et al., 2019) are of some importance. These results illustrate the need to assess retrieval algorithms with MSI radiances simulated by 3D RTMs, for they provide better indications of what to expect once operating with real data.

For demonstration of the radiative closure assessment in the following section, BBR radiances simulated by 3D RTMs, at $\Delta x = 0.25$ km, were averaged up to assessment domains that measure either 5 km across-track by 21 km along-track, denoted as $\mathrm{AD}_{5\times21}$, or 1×21 km, denoted as $\mathrm{AD}_{1\times21}$. The former represent EarthCARE's default domains that are centred on cross-sections of retrieved geophysical variables and include small areas on both sides that are filled by the SCA (Barker et al., 2011; Qu et al., 2023a). This eases the burden of alignment of measurements but also factors into assessments of retrievals results from the SCA. While use of $\mathrm{AD}_{1\times21}$ restricts closure assessments to retrieved cross-sections, which limits the SCA's role to facilitation of, in 3D RTMs, across-track horizontal transport of photons in and out of $\mathrm{AD}_{1\times21}$, assessment credibility might be compromised by requiring BBR measurements to perform outside of its design specifications. Whether to use $\mathrm{AD}_{5\times21}$ or $\mathrm{AD}_{1\times21}$ will be explored during EarthCARE's commissioning phase. Note that while maximum across-track size of an assessment domain is 17 km (for details, see Velázquez Blázquez et al., 2024), that would put far too much emphasis on performance of the SCA.

4 Results

It is instructive to first check on relations between *true* TOA broadband fluxes predicted directly by 3D RTMs and corre-

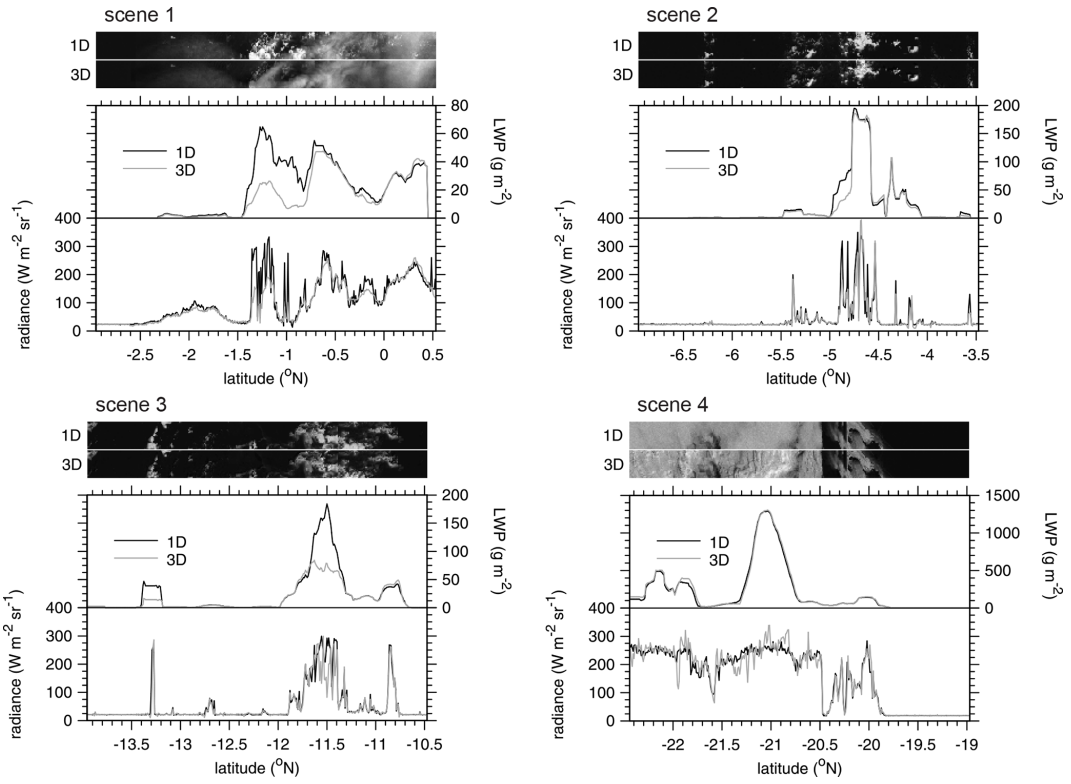

Figure 4. For each $\sim 400 \times 30$ km scene, sampled from the Hawaii frame, top images are MSI 0.67 µm nadir radiances computed using 1D and 3D RTMs. Line plots show 1D and 3D radiances along the centres of the images and corresponding cloud LWP inferred by the CAPTIVATE (ACM-CAP) retrieval algorithm (Mason et al., 2023) when constrained by 1D or 3D MSI radiances. The mean solar zenith angles θ_0 for scenes 1, 2, 3, and 4, are 37, 40, 45, and 51°, respectively.

sponding F_{RTM} based on their simultaneously estimated radiances (see Eqs. 1 and 3). Figure 5 shows these comparisons for SW and LW fluxes for all $\mathrm{AD}_{5\times21}$ in the four scenes; results for $\mathrm{AD}_{1\times21}$ are very similar and not shown. Due to concerns and ambiguities discussed in Sect. 2.2, in addition to F_{RTM} being based on just three radiances, these quantities are not expected to agree perfectly. For cloudless domains with small reflectances and the most reflective overcast domains, values of F_{RTM} agree quite well with their true counterparts. Random deviations are more apparent, often exceeding $\pm 100\,\mathrm{W\,m^{-2}}$, with just a weak tendency for F_{RTM} to underestimate true flux.

As expected, LW values of F_{RTM} agree much better with their true counterparts. This is almost certainly because it is simpler to estimate fluxes based on few radiances for LW radiation than for SW. As alluded to above, the important point here is that because "effective fluxes" for the RTMs are arrived at the same way as they are for BBR measurements, they should provide solid closure assessments that remain as true as possible to ESA's overarching science requirements and objectives.

Figure 6a shows F_{BBR} against F_{RTM} for SW radiation and all $\mathrm{AD}_{1\times21}$. For mostly cloudless conditions, agreement is very good, but as reflectance, and thus cloudiness, increases,

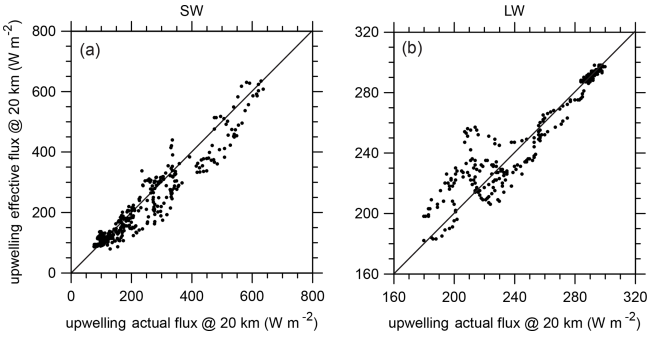

Figure 5. (a) Upwelling effective SW flux at 20 km altitude predicted by Eq. (3) using radiances at three BBR angles against their actual (i.e., hemispheric integrated) counterparts for all $\mathrm{AD}_{5\times21}$ in the four scenes. **(b)** As in panel **(a)** except these are LW quantities.

F_{RTM} becomes increasingly less than F_{BBR} and appears to bifurcate for the most reflective domains with one branch having very poor agreement and the other excellent. At this stage, there are no simple and obvious relations between $F_{\mathrm{RTM}} - F_{\mathrm{BBR}}$ and cloud properties. The objective here, however, was just to demonstrate the methodology and role of the closure process, not to explain retrieval algorithm perfor-

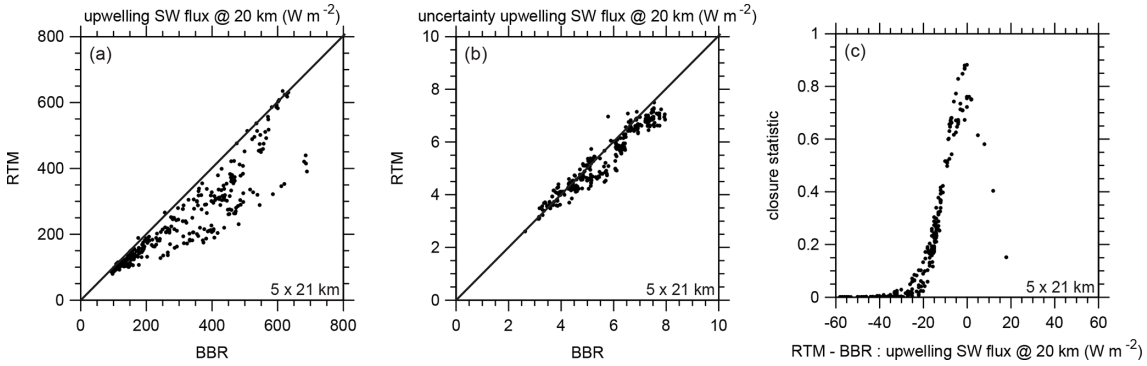

Figure 6. (a) Upwelling effective SW flux at 20 km altitude predicted by Eq. (3) using radiances at three BBR angles based on cloud properties inferred by ACM-CAP against their counterparts based on input cloud properties produced by GEM for all assessment domains $AD_{5\times21}$; the former represent quantities that will come from the ACM-RT process, while the latter represent quantities that will come from the BMA-FLX process using BBR observations. **(b)** Effective SW flux uncertainties that correspond to values in panel **(a)**. **(c)** Closure assessment metric $p_{\Delta\hat{F}}$ using values in panels **(a)** and **(b)** assuming $\Delta\hat{F} = 10\mu_0/\langle\mu_0\rangle\,\mathrm{W\,m^{-2}}$.

mance, that is, for the commissioning phase. Nevertheless, Fig. 6b shows approximate uncertainties of RTM and BBR fluxes to be used in Eq. (6); the former stem from Monte Carlo noise, while the latter stem from errors relative to CERES ADM values. The fact that they are of very comparable magnitude is purely coincidental given the 300 000 photons per domain used in the Monte Carlo RTM. What is clear is that uncertainties are relatively small thanks to the use of effective fluxes that sidestep ADM errors, which can be large for individual domains (e.g., Loeb et al., 2007).

Figure 6c shows $p_{\Delta\hat{F}}$, which is the end of the first step of the closure assessment, based on values shown in Fig. 6a and b. Given the similar flux uncertainties, the assumed Gaussian character of $p_{\Delta\hat{F}}$ is apparent here as a function of ΔF. Moreover, the vast majority of $D_{5\times21}$ have $p_{\Delta\hat{F}} < 0.2$. Even when using $10\mu_0/\langle\mu_0\rangle\,\mathrm{W\,m^{-2}}$, $p_{\Delta\hat{F}}$ only reaches ~ 0.9 on account of σ_p^2 often approaching $10\mu_0/\langle\mu_0\rangle$. This showing differs from that in Illingworth et al. (2015), where many domains showed $p_{\Delta\hat{F}} > 0.75$. The likely explanation for this disparity is that the case in Illingworth et al. (2015) had greater consistency between input and inferred geophysical properties. Namely, inputs were already constrained by CERES radiances, whereas in the present case inputs were defined upfront, and retrievals operated freely as they would with real observations. Note that the archived results using real EarthCARE measurements with reported values of $p_{\Delta\hat{F}}$ for $\Delta\hat{F}$ are between 5 and 50 $\mathrm{W\,m^{-2}}$.

Figure 7 shows the values seen in Fig. 6a and c as a function of latitude along with MSI channel-1 nadir radiances. Note that ACM-CAP retrievals operated on these radiances, in addition to MSI thermal radiances, that were simulated by a 3D RTM. With this small sample it is difficult to discern trends that are worthy of discussion.

Figure 8 shows effective flux uncertainties for BBR and RTM, $\sigma^2_{F_{\mathrm{BBR}}}$ and $\sigma^2_{F_{\mathrm{RTM}}}$, and $p_{\Delta\hat{F}}$ for $AD_{1\times21}$. In general, Monte Carlo flux uncertainties are larger than they are for $AD_{5\times21}$ because the number of injected photons into $AD_{1\times21}$ and their buffer zones is often significantly less than into $AD_{5\times21}$ and their buffer zones (see Cole et al., 2023). The result is a less stringent closure assessment and larger $p_{\Delta\hat{F}}$, to the point of $p_{\Delta\hat{F}} > 0.5$ for some instances of $|\Delta F| > 50\,\mathrm{W\,m^{-2}}$. Note, too, that for $AD_{1\times21}$, errors in RTM fluxes that arise from the SCA, as small as they usually are, do not, unlike for $AD_{5\times21}$, enter explicitly into the assessment, as the assessment domain has collapsed to the retrieved cross-section with the SCA providing boundary conditions only. Nevertheless, it is wise to keep $\sigma^2_{F_{\mathrm{RTM}}}$ as small as resources allow.

Figure 9 shows F_{BBR} against F_{RTM} for LW radiation and all $AD_{5\times21}$. As in Fig. 6a, they agree nicely when fluxes are large, which is for very thin clouds and clear sky. Surprisingly, however, as clouds become thick or more abundant, and as fluxes decrease, RTM radiances resulting from retrievals increasingly exceed BBR radiances. This is surprising despite cloud-top altitudes being placed well via active sensor observations. Nevertheless, differences can be traced to underestimation of high ice cloud water contents.

LW flux uncertainties are often $< 0.5\,\mathrm{W\,m^{-2}}$, which are much less than those for SW fluxes. As Fig. 10 shows, the result is that $p_{\Delta\hat{F}}$ tends to bounce between 0 and 1: the former when cold clouds are missing from retrievals and the latter when only warm low clouds are present (i.e., for the two centre scenes). Clearly there are issues here that must be resolved. While there is the potential luxury here to check retrieved cloud properties against input values, the assessment was cut short to better resemble use of real observations where this luxury does not exist.

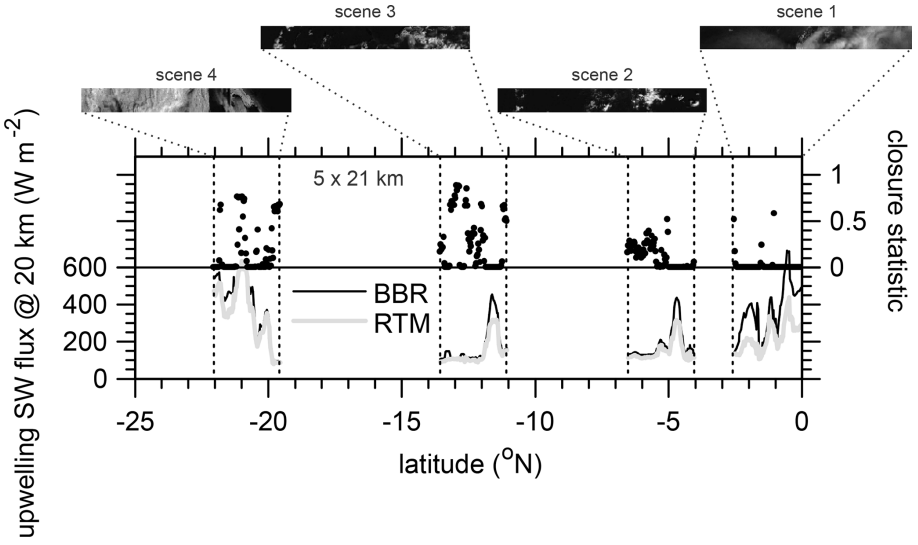

Figure 7. Line plot shows values of upwelling effective SW fluxes at 20 km altitude that are shown in Fig. 6a. Upper portion shows $p_{\Delta\hat{F}}$ values that are shown in Fig. 6c for the four scenes as functions of latitude. MSI channel-1 images, from the 3D RTM, are shown for reference.

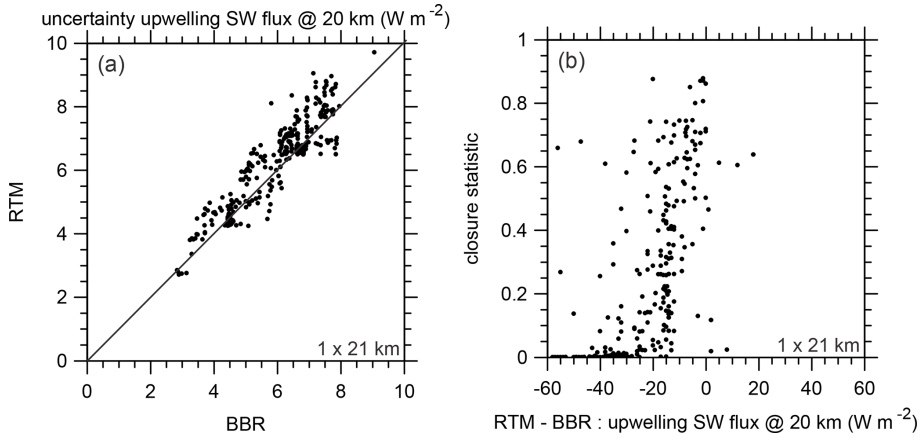

Figure 8. Panels **(a)** and **(b)** are as in Fig. 6b and c except these are for domains $AD_{1\times21}$ that include just the retrieved cross-section.

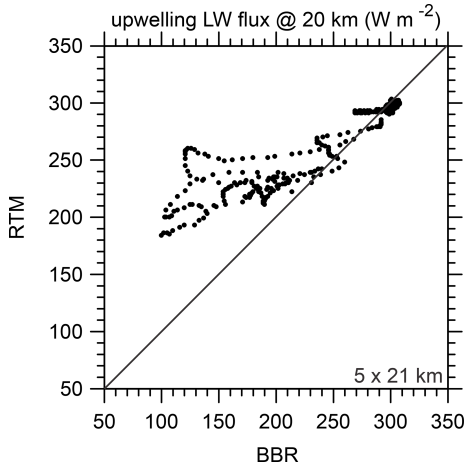

Figure 9. As in Fig. 6a but this is for LW effective fluxes.

5 Summary and discussion

This paper described and demonstrated EarthCARE's planned radiative closure assessment procedure. The assessment's primary objective is to help retrieval algorithm developers diagnose and improve their algorithms during the mission. Second, it is intended to guide users of EarthCARE products who may wish to limit analyses according to performance in the closure assessment. It is important to stress that the intention of this report was *not* to diagnose or assess the quality of retrieval algorithms; that is taking place in other studies, including several in this special issue, and will unfold, post-launch, using real measurements.

From early on in EarthCARE's development, a continuous radiative closure assessment was planned (ESA, 2001). The procedure is conceptually simple: geophysical properties inferred from EarthCARE observations and auxiliary

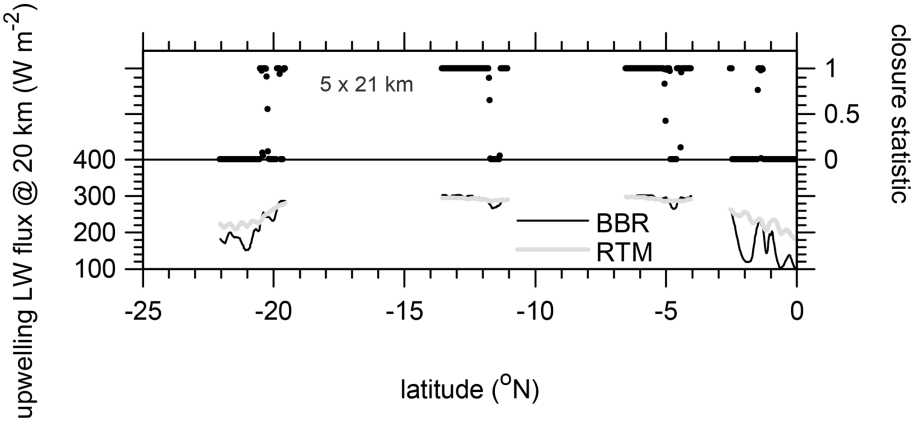

Figure 10. As in Fig. 7 but this is for LW effective fluxes using $\Delta\hat{F} = 10\,\mathrm{W\,m^{-2}}$.

data sources get acted on by broadband radiative transfer models (RTMs), and their results get compared to (near-)simultaneous measurements made by EarthCARE's broadband radiometer (BBR). Crucially, BBR observations are not used by retrieval algorithms. The idea is that when modelled and measured quantities appear *highly likely* to differ by less than $\Delta\hat{F}$, as articulated in the mission's goal (ESA, 2001; Illingworth et al., 2015; Wehr et al., 2023), the retrievals (plus auxiliary input data) are deemed to be *a success*. When, on the other hand, their difference is *too likely* to exceed $\Delta\hat{F}$, developers or users might consider retrievals or auxiliary input data as suspect and in need of addressing, somewhere in the chain (Eisinger et al., 2024), before they pass muster. In this report, the process of assigning a quantitative measure of retrieval performance was explained and demonstrated.

As with most other reports in this special issue, the closure procedure was demonstrated using synthetic EarthCARE observations made by applying a suite of models to simulated atmosphere–surface conditions (Qu et al., 2023b). An important point of departure from all other reports, however, was use of MSI radiances, by retrieval algorithms, and BBR radiances, for flux estimation, that were computed by 3D RTMs; all other reports employed 1D RTM results (Donovan et al., 2023). Obviously, 3D RTMs produce synthetic measurements that better represent satellite measurements. That said, note again that retrieval performance as a function of 1D v. 3D RTM-based synthetic observations was not reported here but will be in forthcoming studies.

The cleanest way to perform a closure assessment is to limit it to observations, which for EarthCARE means BBR radiances. From the outset, however, EarthCARE's goal has been to make cloud and aerosol retrievals that are accurate enough that, when used in RTMs, predicted top-of-atmosphere (TOA) "fluxes" differ from their "observed" counterparts by less than $\Delta\hat{F} = 10\,\mathrm{W\,m^{-2}}$. To remain consistent with this publicly stated goal (ESA, 2001; Illingworth et al., 2015; Wehr et al., 2023), it was decided that the most reliable and inclusive closure methodology would be to transform RTM radiances into "effective fluxes" the same ways that EarthCARE's angular distribution models (ADMs) transform BBR radiances (Velázquez Blázquez et al., 2024). This approach is attractive in that it sidesteps the potentially overwhelming uncertainties associated with single applications of ADMs to small domains and subsequent comparison to ill-defined TOA fluxes produced by 3D RTMs.

Nevertheless, regardless of the variable(s) used, a closure assessment's strength depends directly, and conditionally, on state variables needed by RTMs (e.g., temperature profiles and surface properties). These variables are likely to be outside the purview of mission retrievals, can be highly uncertain, and thus have the potential to seriously compromise the quality and utility of assessments. As the mission unfolds, much attention will be given to quantifying as many uncertainties as possible. Uncertainties associated with EarthCARE's effective fluxes come from the following: minor issues associated with BBR radiances (Velázquez Blázquez et al., 2024), known but approximate errors associated with EarthCARE's ADM (Velázquez Blázquez et al., 2024), and Monte Carlo noise from EarthCARE's 3D RTMs (Cole et al., 2023). Note that large pooled uncertainties (see Eq. 5) for ADM- and RTM-based values of effective flux can appear to improve an assessment by increasing the probability $p_{\Delta\hat{F}}$ that two fluxes differ by less than $\Delta\hat{F}$. Likewise, if uncertainties are underestimated, or worse neglected, retrievals will appear as failures regardless of how little their effective fluxes differ. In other words, in addition to reported likelihoods of effective fluxes differing by less than $\Delta\hat{F}$, users should pay attention to various uncertainties. Particularly insidious are scenarios in which RTMs operate on erroneous, yet assumed to be perfect, inputs, such as surface temperature, albedo, and bidirectional reflectance distribution function that unwittingly yield contaminated TOA radiances and ultimately values of $p_{\Delta\hat{F}}$ that could indicate little about the quality of retrievals.

On a related point, under some conditions cloud evolution and advection can be notable over ~ 3 min, which is the

length of time between forward and backward BBR views. Given the observations at hand, it is almost impossible to reliably quantify how such conditional changes impact estimates of both BBR and RTM effective fluxes. Again, this has the potential to compromise the integrity of closure assessments. Thus far, all simulations of EarthCARE observations have neglected this detail.

Since at least Tornow et al. (2018), it has been the intention to perform radiative closure assessments on domains that measure 5 km across-track by 21 km along-track. Cloud and aerosol properties are, however, retrieved for nadir columns that are ~ 1 km wide. Thus, $\sim 80\,\%$ of each 21 km long assessment domain relies directly on the performance of the scene construction algorithm (SCA) (Barker et al., 2011; Qu et al., 2023a). This is not ideal and gives rise to minor bias errors (see Barker et al., 2014) that can be estimated from MSI radiances (for the tests reported on here, these errors were very minor and not shown). The benefit of 5 km wide domains is that BBR performance should resemble design specs (e.g., Velázquez Blázquez and Clerbaux, 2010). There is the possibility, as shown here, to limit assessment domains to include just the retrieved cross-section, thereby relegating the SCA to purveyor of boundary conditions that enable handling of across-track photon transport by the 3D RTMs. This will, however, stress the performance of the BBR and instrument co-registration. The final decision on domain size, and myriad other issues, will be made during the commissioning phase with the aid of in situ sampling aircraft during collocated flight campaigns.

Code availability. The code used in this study is not currently available but will be made publicly accessible following the official release of the EarthCARE Level 2 processing code by ESA.

Data availability. The results derived from 3D RTM are available from https://doi.org/10.5281/zenodo.11237646 (Barker et al., 2024). The results derived from 1D RTM for the Hawaii scene could be found in the EarthCARE Level-2 demonstration products available from https://doi.org/10.5281/zenodo.7728948 (van Zadelhoff et al., 2023).

Author contributions. HWB drafted the manuscript and developed the methodology presented in this article. JNSC, ZQ, and MK developed several pieces of software that produced data used here. NV developed 3D RT codes and generated all observations based on 3D RTM simulations. AVB and CD developed ADM algorithms that are used to produce effective fluxes. SLM and RJH developed the cloud retrieval algorithm.

Competing interests. The contact author has declared that none of the authors has any competing interests.

Disclaimer. Publisher's note: Copernicus Publications remains neutral with regard to jurisdictional claims made in the text, published maps, institutional affiliations, or any other geographical representation in this paper. While Copernicus Publications makes every effort to include appropriate place names, the final responsibility lies with the authors.

Special issue statement. This article is part of the special issue "EarthCARE Level 2 algorithms and data products". It is not associated with a conference.

Acknowledgements. We are especially indebted to Tobias Wehr, who passed away on 1 February 2023, for his unwavering support and encouragement over many years of work. We also wish to thank Michael Eisinger and all EarthCARE algorithm development team members for their ongoing support, especially Meriem Kacimi (ECCC) and Edward Baudrez (RMIB) for technical help with this study.

Review statement. This paper was edited by Hajime Okamoto and reviewed by two anonymous referees.

References

Barker, H. W., Korolev, A. V., Hudak, D. R., Strapp, J. W., Strawbridge, K. B., and Wolde, M.: A comparison between CloudSat and aircraft data for a multilayer, mixed phase cloud system during the Canadian CloudSat-CALIPSO Validation Project, J. Geophys. Res., 113, D00A16, https://doi.org/10.1029/2008JD009971, 2008.

Barker, H. W., Jerg, M. P., Wehr, T., Kato, S., Donovan, D., and Hogan, R.: A 3D Cloud Construction Algorithm for the EarthCARE satellite mission, Q. J. Roy. Meteor. Soc., 137, 1042–1058, https://doi.org/10.1002/qj.824, 2011.

Barker, H. W., Cole, J. N. S., and Shephard, M.: Estimation of Errors associated with the EarthCARE 3D Scene Construction Algorithm, Q. J. Roy. Meteor. Soc., 140, 2260–2271, https://doi.org/10.1002/qj.2294, 2014.

Barker, H. W., Cole, J. N. S., Domenech, C., Shephard, M., Sioris, C., Tornow, F., and Wehr, T.: Assessing the Quality of Active-Passive Satellite Retrievals using Broadband Radiances, Q. J. Roy. Meteor. Soc., 141, 1294–1305, https://doi.org/10.1002/qj.2438, 2015.

Barker, H. W., Qu, Z., Belair, S., Leroyer, S., Milbrandt, J. A., and Vaillancourt, P. A.: Scaling Properties of Observed and Simulated Satellite Visible Radiances, J. Geophys. Res., 122, 9413–9429, https://doi.org/10.1002/2017JD027146, 2017.

Barker, H., Cole, J., Villefranque, N., Qu, Z., Velazquez-Blazquez, A., Domenech, C., Mason, S., and Hogan, R.: BBR and ACM-RT inputs for figures in ACMB-DF documenting paper (Barker et al., 2024), Zenodo [data set], https://doi.org/10.5281/zenodo.11237646, 2024.

Clerbaux, N., Dewitte, S., Gonzalez, L., Bertrand, C., Nicula, B., and Ipe, A.: Outgoing longwave flux estimation: improvement of angular modelling using spectral information, Remote

Sens. Environ., 85, 389–395, https://doi.org/10.1016/S0034-4257(03)00015-4, 2023a.

Clerbaux, N., Ipe, A., Bertrand, C., Dewitte, S., Nicula, B., and Gonzalez, L.: Evidence of azimuthal anisotropy for the thermal infrared radiation leaving the Earth's atmosphere, Int. J. Remote Sens., 24, 3005–3010, https://doi.org/10.1080/0143116031000106698, 2023b.

Cole, J. N. S., Barker, H. W., Qu, Z., Villefranque, N., and Shephard, M. W.: Broadband radiative quantities for the EarthCARE mission: the ACM-COM and ACM-RT products, Atmos. Meas. Tech., 16, 4271–4288, https://doi.org/10.5194/amt-16-4271-2023, 2023.

Deng, M., Mace, G. G., Wang, Z., and Lawson, R. P.: Evaluation of several A-Train ice cloud retrieval products with in-situ measurements collected during the SPARTICUS campaign, J. Appl. Meteorol. Clim., 52, 1014–1030, https://doi.org/10.1175/JAMC-D-12-054.1, 2013.

Domenech, C. and Wehr, T.: Use of Artificial Neural Networks to Retrieve TOA SW Radiative Fluxes for the EarthCARE Mission, IEEE T. Geosci. Remote, 49, 1839–1849, https://doi.org/10.1109/TGRS.2010.2102768, 2011.

Donovan, D. P., Kollias, P., Velázquez Blázquez, A., and van Zadelhoff, G.-J.: The generation of EarthCARE L1 test data sets using atmospheric model data sets, Atmos. Meas. Tech., 16, 5327–5356, https://doi.org/10.5194/amt-16-5327-2023, 2023.

Eisinger, M., Marnas, F., Wallace, K., Kubota, T., Tomiyama, N., Ohno, Y., Tanaka, T., Tomita, E., Wehr, T., and Bernaerts, D.: The EarthCARE mission: science data processing chain overview, Atmos. Meas. Tech., 17, 839–862, https://doi.org/10.5194/amt-17-839-2024, 2024.

ESA: The Five Candidate Earth Explorer Missions: EarthCARE – Earth Clouds, Aerosols and Radiation Explorer, ESA SP-1257(1), ESA Publications Division: Noordwijk, the Netherlands, ISBN 92-9092-628-7, 2001.

Ham, S.-H., Kato, S., Rose, F. G., Sun-Mack, S., Chen, Y., Miller, W. F., and Scott, R. C.: Combining Cloud Properties from CALIPSO, CloudSat, and MODIS for Top-of-Atmosphere (TOA) Shortwave Broadband Irradiance Computations: Impact of Cloud Vertical Profiles, J. Appl. Meteorol. Clim., 61, 1449–1471, https://doi.org/10.1175/JAMC-D-21-0260.1, 2022.

Henderson, D. S., L'Ecuyer, T., Stephens, G., Partain, P., and Sekiguchi, M.: A Multisensor Perspective on the Radiative Impacts of Clouds and Aerosols, J. Appl. Meteorol. Clim., 52, 853–871, https://doi.org/10.1175/JAMC-D-12-025.1, 2013.

Hogan, R. J., Fielding, M. D., Barker, H. W., Villefranque, N., and Schafer, S. A. K.: Entrapment: An important mechanism to explain the shortwave 3D radiative effect of clouds, J. Atmos. Sci., 76, 2123–2141, https://doi.org/10.1175/JAS-D-18-0366.1, 2019.

Illingworth, A., Barker, H., Beljaars, A., Ceccaldi, M., Chepfer, H., Delanoe, J., Domenech, C., Donovan, D., Fukuda, S., Hirakata, M., Hogan, R., Huenerbein, A., Kollias, P., Kubota, T., Nakajima, T., Nakajima, T., Nishizawa, T., Ohno, Y., and Okamoto, H.: The EARTHCARE satellite: The next step forward in global measurements of clouds, aerosols, precipitation and radiation, B. Am. Meteorol. Soc., 96, 1311–1332, https://doi.org/10.1175/BAMS-D-12-00227.1, 2015.

Kato, S. and Loeb, N. G.: Top-of-atmosphere shortwave broadband observed radiance and estimated irradiance over polar regions from Clouds and the Earth's Radiant Energy System (CERES) instruments on Terra, J. Geophys. Res., 110, D07202, https://doi.org/10.1029/2004JD005308, 2005.

Loeb, N. G., Kato, S., Loukachine, K., Manalo-Smith, N., and Doelling, D. R.: Angular Distribution Models for Top-of-Atmosphere Radiative Flux Estimation from the Clouds and the Earth's Radiant Energy System Instrument on the *Terra* Satellite. Part II: Validation. J. Atmos. Ocean Tech., 24, 564–584, https://doi.org/10.1175/JTECH1983.1, 2007.

Mason, S. L., Barker, H. W., Cole, J. N. S., Docter, N., Donovan, D. P., Hogan, R. J., Hünerbein, A., Kollias, P., Puigdomènech Treserras, B., Qu, Z., Wandinger, U., and van Zadelhoff, G.-J.: An intercomparison of EarthCARE cloud, aerosol, and precipitation retrieval products, Atmos. Meas. Tech., 17, 875–898, https://doi.org/10.5194/amt-17-875-2024, 2024.

Mason, S. L., Hogan, R. J., Bozzo, A., and Pounder, N. L.: A unified synergistic retrieval of clouds, aerosols, and precipitation from EarthCARE: the ACM-CAP product, Atmos. Meas. Tech., 16, 3459–3486, https://doi.org/10.5194/amt-16-3459-2023, 2023.

Qu, Z., Barker, H. W., Cole, J. N. S., and Shephard, M. W.: Across-track extension of retrieved cloud and aerosol properties for the EarthCARE mission: the ACMB-3D product, Atmos. Meas. Tech., 16, 2319–2331, https://doi.org/10.5194/amt-16-2319-2023, 2023a.

Qu, Z., Barker, H. W., Korolev, A. V., Milbrandt, J. A., Wolde, M., Schwarzenböck, A., Leroy, D., Strapp, J. W., Cole, J. N. S., Nguyen, L., and Heidinger, A.: Evaluation of a high-resolution NWP model's simulated clouds using observa-tions from CloudSat and in situ aircraft, Q. J. Roy. Meteor. Soc., 144, 1681–1694, https://doi.org/10.1002/qj.3318, 2018.

Qu, Z., Donovan, D. P., Barker, H. W., Cole, J. N. S., Shephard, M. W., and Huijnen, V.: Numerical model generation of test frames for pre-launch studies of EarthCARE's retrieval algorithms and data management system, Atmos. Meas. Tech., 16, 4927–4946, https://doi.org/10.5194/amt-16-4927-2023, 2023b.

Tornow, F., Barker, H. W., and Domenech, C.: On the use of Simulated Photon Paths to Co-register TOA radiances in *EarthCARE* Radiative Closure Experiments, Q. J. Roy. Meteor. Soc., 141, 3239–3251, https://doi.org/10.1002/qj.2606, 2015.

Tornow, F., Barker, H. W., Velázquez Blázquez, A., Domenech, C., and Fischer, J.: EarthCARE's Broadband Radiometer, 2018: Uncertainties associated with cloudy atmospheres, J. Atmos. Ocean. Tech., 35, 2201–2211, https://doi.org/10.1175/JTECH-D-18-0083.1, 2018.

van Zadelhoff, G.-J. Barker, H. W., Baudrez, E., Bley, S., Clerbaux, N., Cole, J. N. S., de Kloe, J., Docter, N., Domenech, C., Donovan, D. P., Dufresne, J.-L., Eisinger, M., Fischer, J., García-Marañón, R., Haarig, M., Hogan, R., Hünerbein, A., Kollias, P., Koopman, R., Madenach, N., Mason, S. L., Preusker, R., Puigdomènech Treserras, B., Qu, Z., Ruiz-Saldaña, M., Shephard, M., Velázquez-Blazquez, A., Villefranque, N., Wandinger, U., Wang, P., and Wehr, T.: EarthCARE level-2 demonstration products from simulated scenes (10.10), Zenodo [data set], https://doi.org/10.5281/zenodo.7728948, 2023.

Velázquez Blázquez, A., Baudrez, E., Clerbaux, N., and Domenech, C.: Unfiltering of the EarthCARE Broadband Radiometer (BBR) observations: the BM-RAD product, Atmos. Meas. Tech., 17, 4245–4256, https://doi.org/10.5194/amt-17-4245-2024, 2024.

Velázquez Blázquez, A. and Clerbaux, N.: Sensitivity study of the influence of a target spectral signature in the unfiltering process

for broadband radiometers, ESA/ESTEC Final Rep., Contract 22460/09/NL/EL, 102 pp., 2010.

Villefranque, N., Fournier, R., Couvreux, F., Blanco, S., Cornet, C., Eymet, V., Forest, V., and Tregan, J.-M.: A Path-Tracing Monte Carlo Library for 3-D Radiative Transfer in Highly Resolved Cloudy Atmospheres. J. Adv. Model. Earth Sy., 11, 2449–2473, https://doi.org/10.1029/2018MS001602, 2019.

Villefranque, N., Hourdin, F., d'Alençon, L., Blanco, S., Boucher, O., Caliot, C., Coustet, C., Dauchet, J., El Hafi, M., Eymet, V., Farges, O., Forest, V., Fournier, R., Gautrais, J., Masson, V., Piaud, B., and Schoetter, R.: The "teapot in a city": A paradigm shift in urbanclimate modeling, Science Advances, 8, eabp8934, https://doi.org/10.1126/sciadv.abp8934, 2022.

Wehr, T., Kubota, T., Tzeremes, G., Wallace, K., Nakatsuka, H., Ohno, Y., Koopman, R., Rusli, S., Kikuchi, M., Eisinger, M., Tanaka, T., Taga, M., Deghaye, P., Tomita, E., and Bernaerts, D.: The EarthCARE mission – science and system overview, Atmos. Meas. Tech., 16, 3581–3608, https://doi.org/10.5194/amt-16-3581-2023, 2023.